

From an Organic-Functionalized Ge₄S₆ Cage to a Chalcogenidometallate Organic Coordination Framework with Antiferromagnetic Chain Behavior

Zohreh Hassanzadeh Fard,^[a] Rodolphe Clérac,^[b, c] and Stefanie Dehnen^{*,[a]}

The interest in open framework compounds containing chalcogenide building units is due to the intrinsic combination of porosity with further specific chemical or physical properties of the chalcogenide moiety.^[1–7] To date, three different classes of these compounds have been introduced in which chalcogenidometallate complexes or clusters are linked 1) by chalcogenide ligands as in the open framework based on [Cu₅In₃₀S₅₄]^{13–} clusters,^[8] 2) by metal ions as observed in [Sn(Zn₄Sn₄S₁₇)]^{6–},^[9] or 3) by coordinating amines as in [Zn₈S(SC₆H₅)₁₄·C₁₃H₁₄N₂].^[10] The last group represent inorganic–organic hybrid frameworks that add the peculiarities of an organic linker—such as flexibility, chirality or further donor/acceptor capabilities—to the characteristics of the metal chalcogenide fragment—such as optoelectronic properties or magnetism.

Based on the directed synthesis of organic-functionalized chalcogenidometallate complexes, which we have reported very recently,^[11,12] we present a new class of inorganic–organic hybrid compounds, in which inorganic chalcogenidometallate cages (Ge₄S₆) with donor groups (COO[–]) at covalently bonded terminal organic ligands are linked by the coordination of transition-metal ions (Mn²⁺).

The thiogermanate organic coordination framework, [Mn₂{(OOCCH₂Ge)₄S₆}(MeOH)(dmf)₂] (**1**), was synthesized by reaction of the fourfold propionic acid substituted adamantane-type thiogermanate (HOOCC₂H₄Ge)₄S₆

(H₄PAGeS, Figure 1 a) with MnCl₂·4H₂O under solvothermal conditions as colorless crystals (Figure 1 b, c). The structure was determined by single-crystal X-ray diffraction^[13,14] and the complex was also characterized by elemental analysis.

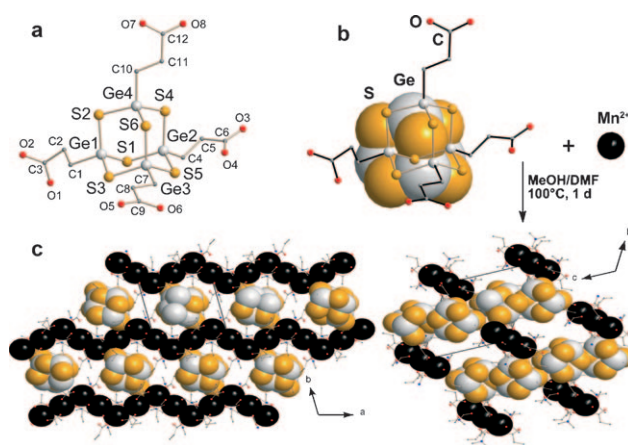


Figure 1. a) Molecular structure of a H₄PAGeS building unit (H atoms not shown). b) Sketch of the reaction H₄PAGeS + Mn²⁺ (Ge, S and Mn atoms in space filling representation) to give c) the three-dimensional framework of **1**, viewed along 001 (left) and 100 (right).

Each asymmetric unit of **1** contains one [(OOCCH₂Ge)₄S₆]^{4–} (PAGeS) adamantane cage, two Mn²⁺ ions (on three crystallographic sites), one coordinated methanol and two coordinated DMF molecules. The PAGeS cage is linked to eight Mn atoms (Figure 2 a): the propionic acid substituent at Ge1 coordinates to three Mn (Mn1–Mn3) atoms at once in a η²–μ,μ bridging mode, whereas the COO[–] group at Ge2 is just a monodentate ligand to Mn2 with the second O atom (O4) being uniquely non-coordinating. The two donor atoms at each of the ligands at Ge3 and Ge4 serve to connect Mn1 with Mn2. Hence, the three crystallographically independent Mn atoms exhibit different local coordination environments (Figure 2 b). Mn1 is octahedrally coordinated by one of the O atoms of six different PAGeS

[a] Z. Hassanzadeh Fard, Prof. Dr. S. Dehnen
Fachbereich Chemie und
Wissenschaftliches Zentrum für Materialwissenschaften (WZMW)
Philipps-Universität Marburg, Hans-Meerwein Strasse
35043 Marburg (Germany)
Fax: (+49) 6421-282-5653
E-mail: dehnen@chemie.uni-marburg.de

[b] Prof. Dr. R. Clérac
CNRS, UPR 8641, Centre de Recherche Paul Pascal (CRPP)
Equipe “Matériaux Moléculaires Magnétiques”
115 Avenue du Dr. A. Schweitzer, 33600 Pessac (France)

[c] Prof. Dr. R. Clérac
Université de Bordeaux, UPR 8641, 33600 Pessac (France)

Supporting information for this article is available on the WWW under <http://dx.doi.org/10.1002/chem.200902921>.

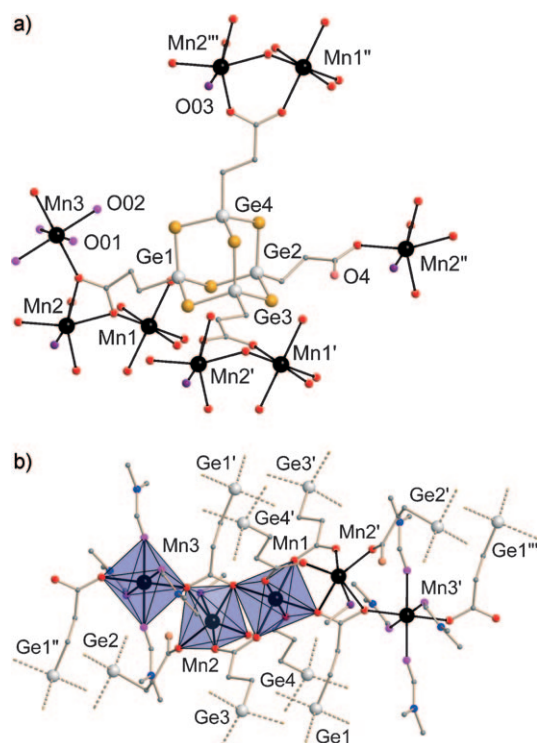


Figure 2. a) Coordination of the PAgES unit to eight Mn²⁺ ions. b) Coordination environments of the three Mn centers by O donor atoms of COO⁻ groups (red), DMF (pink) or MeOH molecules (violet).

complexes, which are in turn linked by this single metal atom, whereas the second O atoms of the same COO⁻ groups are always involved in further coordination. Mn2 shows a complicated, distorted octahedral coordination by two O atoms of the chelating ligand at Ge1, three further PAgES in a monodentate fashion, and one MeOH molecule. Mn3 is mono-coordinated by two PAgES units in *trans*-position and four terminal DMF molecules.

The linkage of PAgES cages as one secondary building unit (SBU-1) and Mn atoms results in the formation of one-dimensional zigzag chains of corner-sharing {MnO₆} units along the crystallographic *a* axis at *a*00, *a*10, *a*01, and *a*11. The PAgES cages are distributed between the {MnO₆}_x chains and bind to four independent zigzag chains each, producing a highly intertwined three-dimensional network. In detail, Mn2, Mn1, and Mn2' form a carboxylate-bridged, trimeric linear SBU-2, which is bridged by DMF-coordinated Mn3 as a biconnector into the zigzag chain. Beside this linkage, each trimeric SBU-2 binds to eight adamantane SBU-1s to achieve an 8+2=10 connectivity. Each SBU-1, in turn, is connected to four of the SBU-2 trimeric aggregates. Thus **1** exhibits a novel (4,10)-connected three-dimensional network topology.

UV/Vis spectra served to explore the electronic excitation energy. Figure 3 shows the spectrum that was recorded from a suspension of single crystals of **1** in nujol oil.

In accordance with the colorless crystals, the electronic excitation of **1** is situated in the UV region. However, one

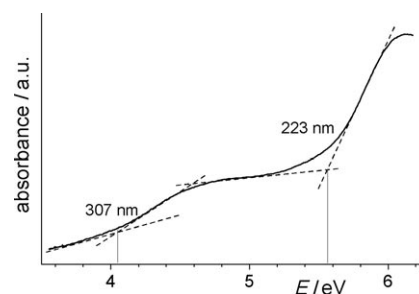


Figure 3. UV/Vis spectrum of **1**, recorded from a suspension of single crystals in nujol oil.

can clearly distinguish between two onsets of absorption (Figure 3). The first (4.04 eV) can be assigned to the p(O)→d(Mn) charge transfer as typical for carboxylate ligated {MnO₆} arrangements;^[15] the second (5.57 eV) can be assigned to the p(S)→p(Ge) CT excitation, similar to the absorption observed for organic ligated R₄Ge₄S₆.^[16] This illustrates that the hybrid compound **1** contains different electronic domains. Modifications, such as the use of thiocarboxylate ligands and/or different transition metal atoms, will serve to additionally fine-tune these properties as observed for purely inorganic chalcogenidometallate networks.^[5,6]

Magnetic susceptibility measurements have been performed on **1** at 1000 Oe between 1.8 and 300 K. At room temperature, the χT product is 16.7 cm³ K mol⁻¹, in good agreement with the presence of four *S*=5/2 Mn^{II} spins. The value of χT decreases continuously with *T* to reach 2.85 cm³ K mol⁻¹ at 1.8 K, indicating the presence of dominating antiferromagnetic (AF) interactions along the Mn chain. In order to model the magnetic properties of **1**, the crystal structure was analyzed by localizing the possible magnetic pathways. Three different magnetic interactions were identified along the Mn chain: 1) *J*₁ between Mn1 and Mn2 bridged by two *syn-syn* carboxylates and μ -O1 (Mn1-O1-Mn2 110.94(18)°); 2) *J*₂ between Mn2 and Mn3 linked by a single μ -O2 (Mn2-O2-Mn3 138.48(19)°); and 3) *J*₃ mediated by a single *anti-anti* carboxylate between Mn1 and Mn3. According to the literature,^[17] *J*₁ should represent the strongest AF interaction due to the two *syn-syn* carboxylate bridges, being reinforced by the μ -O1 link. *J*₂ and *J*₃ should be much smaller, most likely with $|J_2| > |J_3|$ due to the direct orbital overlap through μ -O2 for *J*₂ and the *anti-anti* carboxylate bridge for *J*₃, which is usually extremely weak being ferro- or antiferromagnetic by nature.^[17b,18] A simple Heisenberg trinuclear *S*=5/2 model, taking into account only *J*₁ (with the spin Hamiltonian: $H = -2JS_{\text{Mn1}}(S_{\text{Mn2}} + S_{\text{Mn2}'})$) and neglecting the other pathways (i.e., considering the Mn3 spin as Curie spin), was not able to reproduce the experimental data below 50 K. Therefore, as a second approach the interaction *J*₁ and *J*₂ were included in the model (still neglecting the weaker *J*₃ interaction) as a *J*₁*J*₂ interaction sequence between *S*=5/2 spins (inset of Figure 4). The following Heisenberg classical spin Hamiltonian was considered [Eq. (1)].

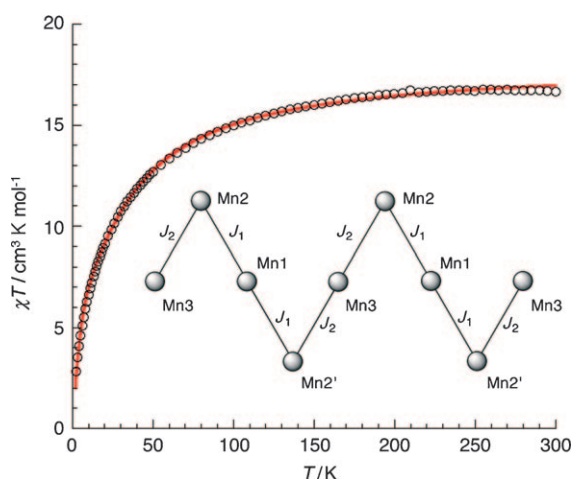


Figure 4. χT vs. T plot for **1** at 1000 Oe (χ : magnetic susceptibility defined as M/H per four Mn^{II} sites). The solid red line is the best fit obtained with the $J_1J_2J_3$ Heisenberg chain model described in the text. Inset: magnetic topology of the Mn chain.

$$H = -2 \left\{ \sum_{i=0}^N J_1 (S_{4i+1} \cdot S_{4i+2} + S_{4i+2} \cdot S_{4i+3}) + J_2 (S_{4i+3} \cdot S_{4i+4} + S_{4i+4} \cdot S_{4i+5}) \right\} \quad (1)$$

The work of Fisher^[19] was extended in order to calculate the magnetic susceptibility of this system [Eq. (2)] in which u_i is given by Equation (3).

$$\chi T = \frac{2Ng^2\mu_B^2S(S+1)}{3k_B} \left[\frac{2(u_1 + u_2) + (u_1 + u_2)^2 + 2(1 + u_1^2u_2 + u_1u_2^2 + u_1^2u_2^2)}{1 - u_1^2u_2^2} \right] \quad (2)$$

$$u_i = \left(\tanh \left(\frac{2J_iS(S+1)}{k_BT} \right) \right)^{-1} - \frac{k_BT}{2J_iS(S+1)} \quad (3)$$

As shown in Figure 4, an excellent fit of the data is obtained with $J_1/k_B = -2.8(2)$ K, $J_2/k_B = -0.3(1)$ K, and $g = 2.03(5)$. The estimation of the magnetic interactions is in excellent agreement with the previously reported values.^[18,19] A more complicated model taking into account J_3 led to an overparametrization of the fit (with multiple solutions) and meaningless magnetic parameters.

In conclusion we have presented a novel type of hybrid compound based on organic-functionalized metalchalcogenide cages as well as transition-metal ions as nodes, both of which contribute to the electronic situation and thus the properties of the network.

Experimental Section

General: All manipulations steps were performed under an Ar atmosphere. All solvents were dried and freshly distilled prior to use.

H₄PAGeS was prepared according to the reported method.^[12] MnCl₂·4H₂O was purchased from Aldrich (>98%) and used as received.

Synthesis of [Mn₂((OCC₂H₄Ge)₄S₆)(MeOH)(dmf)₂] (1**):** H₄PAGeS (0.01 g, 0.013 mmol) and MnCl₂·4H₂O (0.004 g, 0.0195 mmol) were placed in a pyrex glass tube (10 mm diameter and 200 mm length) in a solvent mixture of DMF/methanol (0.3/0.2 mL). The tube was sealed under vacuum and heated at a constant rate of 1°Cmin⁻¹ to 100°C for 24 h, then cooled at a constant rate of 0.5°Cmin⁻¹ to room temperature. The colorless crystals of **1** were washed with methanol repeatedly (5 × 2 mL). Yield: 0.006 g (0.0056 mmol, 43%); FT-IR (KBr, Nujol mull in polyethylene windows): $\tilde{\nu}$ = 3418.1 (br, methanol OH), 2921.7 (w), 1655.5 (s, DMF C=O), 1565.7 (s, COO asymmetric stretch), 1400.3 (s, COO symmetric stretch), 1299.8 (m, CN), 1255.3 (w), 1168.0 (w), 1106.4 (m), 778.9 (m), 709.0 (w), 424.4 (s, GeS), 381.0 (w), 315.0 (w), 195.4 (w), 153.2 cm⁻¹ (w); UV/Vis (suspension of single crystals in nujol oil): λ_{\max} (ε) = 307–(4.04), 223 nm (5.57 eV); elemental analysis calcd (%): C 21.40, H 3.33, N 2.62, S 17.96; found: C 21.36, H 3.30, N 2.62, S 18.00.

Acknowledgements

This work was financially supported by the Deutsche Forschungsgemeinschaft (DFG), MAGMANet (NMP3-CT-2005-515767), the “Région Aquitaine”, GIS Advanced Materials in Aquitaine (COMET Project), the ANR, the University of Bordeaux and the CNRS. We are very indebted to Prof. Dr. D. Proserpio for his help with the analysis of the network topology.

Keywords: chalcogens • magnetic properties • manganese • organic–inorganic hybrid composites • solvothermal conditions

- [1] a) Z. Zhang, J. Zhang, T. Wu, X. Bu, P. Feng, *J. Am. Chem. Soc.* **2008**, *130*, 15238–15239; b) N. Zheng, X. Bu, P. Feng, *J. Am. Chem. Soc.* **2005**, *127*, 5286–5287; c) P. Feng, X. Bu, N. Zheng, *Acc. Chem. Res.* **2005**, *38*, 293–303.
- [2] F. E. Osterloh, *Chem. Mater.* **2008**, *20*, 35–54.
- [3] a) H. Li, J. Kim, T. L. Groy, M. O’Keeffe, O. M. Yaghi, *J. Am. Chem. Soc.* **2001**, *123*, 4867–4868; b) H. Li, A. Laine, M. O’Keeffe, O. M. Yaghi, *Science* **1999**, *283*, 1145–1147.
- [4] a) C. L. Cahill, J. B. Parise, *J. Chem. Soc. Dalton Trans.* **2000**, 1475–1482; b) C. L. Cahill, Y. Ko, J. B. Parise, *Chem. Mater.* **1998**, *10*, 19–21.
- [5] a) M. J. Manos, J. I. Jang, J. B. Ketterson, M. G. Kanatzidis, *Chem. Commun.* **2008**, 972–974; b) N. Ding, M. G. Kanatzidis, *Chem. Mater.* **2007**, *19*, 3867–3869; c) S. Bag, P. N. Trikalitis, P. J. Chupas, G. S. Armatas, M. G. Kanatzidis, *Science* **2007**, *317*, 490–493.
- [6] a) S. Haddadpour, M. Melullis, H. Staesche, C. R. Mariappan, B. Roling, R. Clérac, S. Dehnen, *Inorg. Chem.* **2009**, *48*, 1689–1698; b) S. Dehnen, M. Melullis, *Coord. Chem. Rev.* **2007**, *251*, 1259–1280; c) M. K. Brandmayer, R. Clérac, F. Weigend, S. Dehnen, *Chem. Eur. J.* **2004**, *10*, 5147–5157.
- [7] a) P. Vaqueiro, *Inorg. Chem.* **2008**, *47*, 20–22; b) P. Vaqueiro, M. L. Romero, *Chem. Commun.* **2007**, 3282–3284.
- [8] X. Bu, N. Zheng, Y. Li, P. Feng, *J. Am. Chem. Soc.* **2002**, *124*, 12646–12647.
- [9] M. J. Manos, R. G. Iyer, E. Quarez, J. H. Liao, M. G. Kanatzidis, *Angew. Chem.* **2005**, *117*, 3618–3621; *Angew. Chem. Int. Ed.* **2005**, *44*, 3552–3555.
- [10] N. Zheng, X. Bu, P. Feng, *J. Am. Chem. Soc.* **2002**, *124*, 9688–9689.
- [11] Z. Hassanzadeh Fard, L. Xiong, C. Müller, M. Holyńska, S. Dehnen, *Chem. Eur. J.* **2009**, *15*, 6595–6604.

- [12] Z. Hassanzadeh Fard, C. Müller, T. Harmening, R. Pöttgen, S. Dehnen, *Angew. Chem.* **2009**, *121*, 4507–4511; *Angew. Chem. Int. Ed.* **2009**, *48*, 4441–4444.
- [13] Data collection on Stoe IPDS2T (Mo $\text{K}\alpha$ radiation, graphite monochromization, $\lambda=0.71073$ Å, 100 K). Structure solution by direct methods, full-matrix-least-squares refinement on F^2 by using SHELXTL software.^[14] C_{19.09}H_{35.36}Ge₄Mn₂N₂O_{11.59}S₆ (**1**): triclinic, $P\bar{1}$, $a=12.311(3)$, $b=14.049(3)$, $c=14.181(3)$ Å, $\alpha=116.92(3)^\circ$, $\beta=111.72(3)^\circ$, $\gamma=91.66(3)^\circ$, $V=1973.6(7)$ Å³, $Z=2$. $R1=0.0542$ [$I>2\sigma(I)$], $wR2=0.0988$ (all data), $GOF=0.969$. For more details, see the Supporting Information. CCDC-746886 contains the supplementary crystallographic data for compound **1** in this paper. These data can be obtained free of charge from The Cambridge Crystallographic Data Centre via www.ccdc.cam.ac.uk/data_request/cif.
- [14] SHELXTL 5.1, G. M. Sheldrick, Bruker AXS Inc., Madison, **1997**.
- [15] S. M. Oppenheimer, A. B. Sushkov, J. L. Musfeldt, R. M. Achey, N. S. Dalal, *Phys. Rev. B* **2002**, *65*, 054419.
- [16] M. Unno, Y. Kawai, H. Shioyama, H. Matsumoto, *Organometallics* **1997**, *16*, 4428–4434.
- [17] See for example: a) R. Wang, D. Yuan, F. Jiang, L. Han, S. Gao, M. Hong, *Eur. J. Inorg. Chem.* **2006**, 1649–1656, and references therein; b) S. Durot, C. Policar, G. Pelosi, F. Bisceglie, T. Mallah, J. P. Mahy, *Inorg. Chem.* **2003**, *42*, 8072–8080, and references therein.
- [18] a) E. Colacio, J. M. Domínguez-Vera, M. Ghazi, R. Kivekäs, M. Klinga, J. M. Moreno, *Eur. J. Inorg. Chem.* **1999**, 441–445 and references therein; b) C. Ruiz-Pérez, M. Hernandez-Molina, P. Lorenzo-Luis, F. Lloret, J. Cano, M. Julve, *Inorg. Chem.* **2000**, *39*, 3845–3852.
- [19] M. E. Fisher, *Am. J. Phys.* **1964**, *32*, 343–346.

Received: October 22, 2009
Published online: January 15, 2010